The Role of Chemical Structure in Indacenodithienothiophene-alt-Benzothiadiazole Copolymers for High Performance Organic Solar Cells With Improved Photo-Stability Through Minimization of Burn-in Loss

Christos L. Chochos, Nicolas Leclerc, Nicola Gasparini, Nicolas Zimmermann, Elisavet Tatsi, Athanasios Katsouras, Dimitrios Moschovas, Efthymis Serpetzoglou, Ioannis Konidakis, Sadiara Fall, et al.

Journal of Materials Chemistry A

Accepted Manuscript

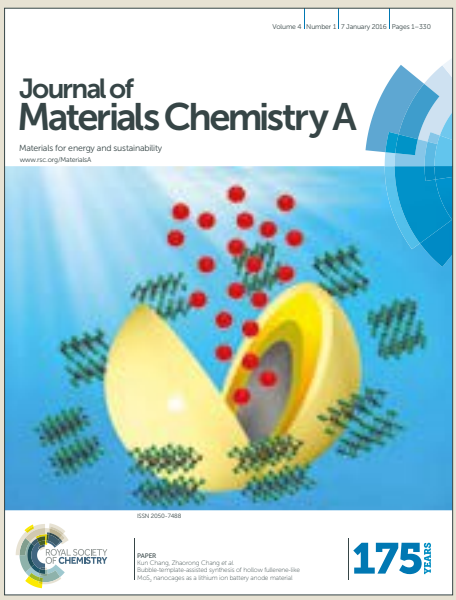

ROYAL SOCIETY OF CHEMISTRY

rsc.li/materials-a

View Article Online
DOI: 10.1039/C7TA09224E

View Article Online
DOI: 10.1039/C7TA09224E

The Role of Chemical Structure in Indacenodithienothiophene-*alt*-Benzothiadiazole Copolymers for High Performance Organic Solar Cells With Improved Photo-Stability Through Minimization of Burn-in Loss

Christos L. Chochos,[a,b]* Nicolas Leclerc,[c]* Nicola Gasparini,[d]* Nicolas Zimmerman,[e] Elisavet Tatsi,[a] Athanasios Katsouras,[a] Dimitrios Moschovas,[a] Efthymis Serpetzoglou,[f] Ioannis Konidakis,[f] Sadiara Fall,[e] Patrick Lévêque,[e] Thomas Heiser,[e] Michael Spanos,[a,g] Vasilis G. Gregoriou,[b,g] Emmanuel Stratakis,[f] Tayebeh Ameri,[d] Christoph J. Brabec,[d,h] Apostolos Avgeropoulos[a]*

[a] Department of Materials Science Engineering, University of Ioannina, Ioannina 45110, Greece

[b] Advent Technologies SA, Patras Science Park, Stadiou Street, Platani-Rio, 26504, Patra, Greece

[c] Université de Strasbourg, CNRS, ICPEES, UMR 7515, F67087 Strasbourg, France

[d] Institute of Materials for Electronics and Energy Technology (I-MEET), Friedrich-Alexander-University Erlangen-Nuremberg, Martensstraße 7, 91058 Erlangen, Germany

[e] Université de Strasbourg, CNRS, ENGEES, INSA, ICube UMR 7357, F-67000 Strasbourg, France

[f] Institute of Electronic Structure and Laser, Foundation for Research and Technology – Hellas, P. O. Box 1527, Heraklion, Crete, Greece

[g] National Hellenic Research Foundation (NHRF), 48 Vassileos Constantinou Avenue, Athens 11635, Greece

[h] Bavarian Center for Applied Energy Research (ZAE Bayern), Haberstrasse 2a, 91058 Erlangen, Germany

*E-mail addresses cchochos@cc.uoi.gr; cchochos@advent-energy.com; leclercn@unistra.fr; nicola.gasparini@fau.de; aavger@cc.uoi.gr

View Article Online
DOI: 10.1039/C7TA09224E

Abstract

It is of outmost importance to gain in depth understanding on the role of the polymer chemical structure in the corresponding organic solar cell (OSC) performance and degradation behavior that is insufficiently explored. Achieving these correlations it will set new design rules towards further optimization of polymer chemical structures for OSCs with high performances and long stability. In this study, our efforts have been focused to identify how the nature of aryl substituents and the number of fluorine atoms anchored in the backbone of indacenodithieno[3,2-*b*]thiophene (IDTT) based polymers influence their optoelectronic properties, the OSC performances and the degradation mechanisms. The most important outcome of this study is the demonstration that standard initial burn-in loss is primary attributed to microstructure instabilities. Furthermore, the initial burn-in loss could be substantially reduced through the rational design of the polymeric semiconductor's chemical structure, leading to improved lifetimes and low (20%) initial power conversion efficiency loss. In particular, we identify the beneficial effect of the presence of the two fluorine atoms on the benzo[*c*][1,2,5]thiadiazole (BTD), as compared to the non-fluorinated and mono-fluorinated analogues, in decreasing the burn-in by reducing the microstructure instabilities regardless of the aryl substituent that is present in the polymer backbone.

Keywords: organic solar cells, stability, Donor-Acceptor conjugated polymers, burn-in, structure-property relationships

† Electronic supplementary information (ESI) available: Synthesis, gel permeation chromatography, absorption spectroscopy and cyclic voltammetry characterisation of the polymers. Fabrication and characterisation of organic solar cells, transport characteristics and transient absorption spectroscopy of the devices. High resolution transmission electron microscopy and micro-RAMAN spectroscopy. See DOI: 10.1039/…….

View Article Online
DOI: 10.1039/C7TA09224E

1. Introduction

It is becoming increasingly clear that systematic optimization of the chemical structure of "donor-acceptor" (D-A) polymeric semiconductors as electron donors in organic photovoltaics (OPVs) is a challenging task for which accurate guidelines are yet to be determined.[1] Several different structural and molecular parameters are crucial ingredients for obtaining polymeric semiconductors that simultaneously possess high power conversion efficiencies (PCEs), easy processability in common organic solvents and enhanced stability in OPVs. Although the PCE of OPV devices has been considerably improved to over 12%,[2] their stability (or lifetime) is still too poor to consider the aspect of large commercialization.[3]

Even though, a large number of new conjugated polymers have been synthesized, most of the published manuscripts up to date have been focused solely on the structure – performance relationship towards high efficiency while neglecting structure – stability relationship.[2,4] The result is that despite their potential and scientific interest, many of the active materials based on these compounds may not be useful for real world applications. Among various factors that affecting the stability of polymer:fullerene solar cells, light, heat, oxygen, and humidity are the essential considerations.[5] While the effect of oxygen and humidity can be suppressed by proper encapsulation,[6] light and accumulated heat from illumination are inherently unavoidable and must be addressed with the highest priority. The active layer component in the organic solar cell is the part of the device that is very sensitive to light and heat[5] and since it is integral to the device's functionality this translates directly into a degradation of the PCE.

In general, many organic molecules and polymers are by nature sensitive to photo-oxidation upon exposure to light as evidenced by the poly-phenylenevinylene (PPV) type polymers that were used in the early days of OPV research. The photochemical decomposition of the PPV type polymer has

View Article Online
DOI: 10.1039/C7TA09224E

shown to involve both side chain degradation, and also attack at the vinylene moieties.[7] Polyfluorenes that are used as blue emitters in OLEDs, have shown to be prone to oxidation giving rise to an unwanted green emission. It has long been known that the end-product of the oxidation at the 9-position of fluorene is to produce fluorenone units.[8] Poly(3-hexyl-thiophene) (P3HT) is degraded through a side chain oxidation starting with a hydroperoxide formation at the benzylic position, but as compared to PPV and polyfluorene derivatives it is found to be orders of magnitude more stable,[9] allowing the development of roll-to-roll (R2R) processing.[10]

The current generation of conjugated polymers (mostly based on D-A alternated polymers), exhibit a larger degree of intrinsic stability but is still highly susceptible to photo-oxidation when exposed to sunlight and air. However, the photo-stability of a large number of these D-A polymers has been investigated by various groups and photo-stable polymer design guidelines have been suggested.[11] For example, electron-rich units with side chains are the most susceptible to degradation; especially the fluorene and cyclopentadithiophene moieties impart low stability.[11a] The most stable donor monomers are clearly those without side chains. Though only one example is shown, it is interesting to note that substituting a carbon with silicon as the atom for attachment of the side groups, this increases the stability significantly.[11a] The presence of fluorine atom(s) in aromatic small molecules also contributes in the improvement of photo-stability.[11d,e] Finally, polymeric materials with higher degree of crystallinity are shown to be more resistant to photo-oxidation.[11b,c]

Although such observations are promising, a more fundamental understanding of photo-degradation processes that lead to short-term burn-in[5b,12] and long-term performance loss[5b] is still needed. For this reason, it is of outmost importance to conduct extensive photo-stability studies in more real working conditions, e.g. OPV devices and not solely to neat polymeric films. Up to now, these kind of studies are very few and limited, but in principal they can lead to more reliable and

View Article Online
DOI: 10.1039/C7TA09224E

accurate conclusions in order to address the impact of light on the long term stability issue of OPVs.[13]

Taking these into consideration, in this contribution, our efforts towards the establishment of a structure-photophysical properties-OPV performance and OPV long-term stability correlation has been accomplished in terms of aromatic substituents optimization and fluorine content in a family of high bandgap (HBG) alternating conjugated polymers consisting of indacenodithieno[3,2-*b*]thiophene (IDTT) as the electron donating unit and benzo[*c*][1,2,5]thiadiazole (BTD) as the electron withdrawing building block in the polymer backbone. In order to achieve this, we examine the influence of anchoring two different aryl substituents (phenyl and thienyl) on the IDTT and introduce one or two fluorine atom(s) onto the BTD. Our design concept was based on the fact that IDTT-based D-A conjugated polymers have demonstrated great promise as *p*-type polymers in OPVs.[14] In fact, *Jen et al*. reported a D-A polymer based on IDTT and difluoro-BTD with a PCE of 7%,[14a] whereas upon addition of plasmonics the PCE increased to 9.2%.[14b] However, a systematic study regarding the structure-photophysical properties-OPV performance for this type of D-A polymers is missing.

Moreover, taking into account the polymer design guidelines that have been reported previously for enhanced photo-stability, formation of highly planar backbone conformation could be expected for the new synthesized conjugated polymers, due to the presence of IDTT and BTD, through the synergistic effects of the tight π-π stacking and the non-covalent interactions which possibly will lead to better ordering of the polymer chains and as a consequently to increase the degree of crystallinity. In addition, the weak donating strength of IDTT results in conjugated polymers with deep-lying highest occupied molecular orbital energy levels (E_{HOMO}),[14c,d,g] a parameter which should benefit oxidative stability[15] and lead to high V_{oc} in photovoltaic devices. Finally, the insertion of one or two fluorine atom(s) on the BTD along with the direct anchoring of aromatic

View Article Online
DOI: 10.1039/C7TA09224E

substituents instead of alkyl side chains on the IDTT (we maintain the presence of alkyl side chains on the aryl substituents at the periphery of IDTT to the minimum length and density in order to obtain sufficient solubility in organic solvents) can contribute not only to the improved photo-stability of the new synthesized polymers but also to the PCE increase, in particular through the π-stacking strengthening.[16]

2. Results and Discussion

2.1 Synthesis

The polymers were synthesized by the Stille aromatic cross-coupling polymerization[17] utilizing tris(dibenzylideneacetone)dipalladium(0) [$Pd_2(dba_3)$] in 2% per mole and tri(*o*-tolyl)phosphine [$P(o\text{-tol})_3$], 8% per mole, as the catalytic system in toluene solution as shown in Scheme 1. In order to achieve the structure-photophysical properties-OPV performance and stability study in terms of IDTT's aryl substitution and number of fluorine atoms in the BTD, the bis(trimethylstannyl)tetrahexylphenyl-IDTT (M1) or the bis(trimethylstannyl)tetrahexylthienyl-IDTT (M2) were combined with the 4,7-dibromobenzo[*c*][1,2,5]thiadiazole (M3) to provide CTL1 and CTL4 or with the 4,7-dibromo-5-fluorobenzo[*c*][1,2,5]thiadiazole (M4) to afford CTL2 and CTL5 and finally with the 4,7-dibromo-5,6-difluorobenzo[*c*][1,2,5]thiadiazole (M5) to give the CTL3 and CTL6, respectively.

After purification, using Soxhlet extraction, CTL1-3, CTL5 and CTL6 are received from the chlorobenzene (CB) fraction, whereas CTL4 is obtained from the chloroform (CF) fraction. The average molecular weights per number ($\overline{M_n}$), per weight ($\overline{M_w}$) and dispersity ($Đ$) of the polymers as measured by gel permeation chromatography (GPC) based on monodispersed polystyrene standards at high temperature (150 °C) and utilizing ortho-dichlorobenzene (*o*-DCB) as eluent (more details in the experimental section) are shown in Figure S1 [in the Supporting Information

View Article Online
DOI: 10.1039/C7TA09224E

(SI)] and are summarized in Table S1 (SI). It is shown that the polymers present monomodal GPC profiles with no appearance of residual monomers or oligomer chains. Moreover, the CTL1-3, containing the phenyl substituents on the IDTT, exhibit extremely high $\overline{M_n}$ ranging from 65300 to 182500 g/mol which gradually decreases as the number of the fluorine atoms on the BDT increases. On the other hand, the CTL4-6, containing the thienyl substituents on the IDTT, exhibit significantly lower $\overline{M_n}$, as compared to CTL1-3, ranging from 13150 to 36700 g/mol. However, in this case, the $\overline{M_n}$ gradually increases as the number of the fluorine atoms on the BDT increases. It should be noted that the $\overline{M_n}$ of CTL3 reported in this work is significantly higher than in a recently published study[14a] but with increased $Đ$. The $Đ$ for the other polymers (CTL1, CTL2 and CTL4-6) ranges between 2.1 and 3.3.

Scheme 1 Chemical structures of the studied conjugated polymers CTL1-6.

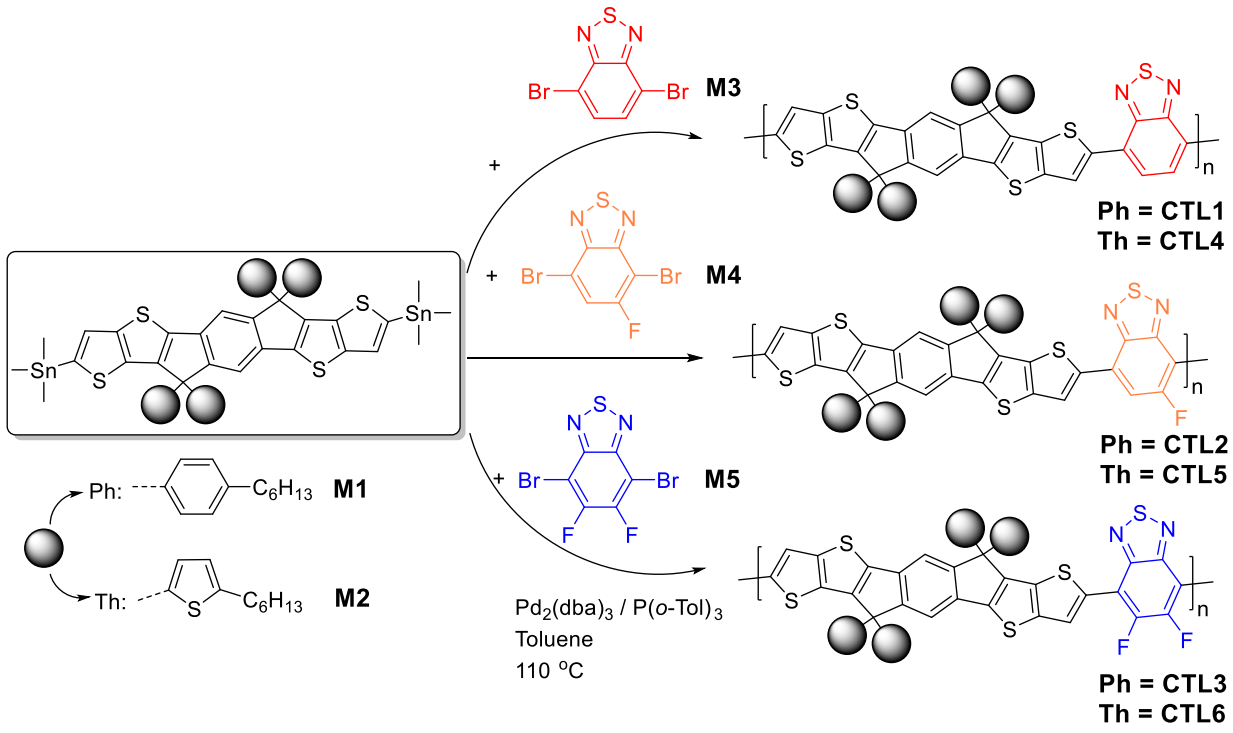

2.2 Optical and electrochemical properties

View Article Online
DOI: 10.1039/C7TA09224E

The absorption spectra of the copolymers CTL1-6 in *o*-DCB solution and as thin films are presented in Figure S2 in SI, and the corresponding optoelectronic properties are summarized in Table 1. All polymers display qualitatively similar spectral shape. For each polymer, two major absorption bands are observed in solution (Figure S2a); a feature that is commonly observed for alternating D-A copolymers. The low-wavelength peak is attributed to a delocalized π-π* transition while the high-wavelength transition is related to an intramolecular D-A charge transfer.[18] In general, it is demonstrated that the absorption peak maxima of both the high- and low- energy transitions of the CTL1-3, containing the phenyl substituents on the IDTT, are red shifted as compared to CTL4-6, containing the thienyl substituents on the IDTT, independent of the number of fluorine atoms on the BTD (Table 1). Furthermore, comparing CTL1, CTL2 and CTL3 it is shown that addition of one fluorine atom on BTD (CTL2) does not alter the absorption maxima of both the high- and low- wavelength peaks of CTL1 (unsubstituted BTD). As usually observed, further addition of fluorine atom on the BTD (CTL3), results to the blue shift of the high wavelength absorption maxima as compared to CTL1 and CTL2, without affecting significantly the low wavelength absorption maxima, though (Table 1).[16] A similar trend is also observed for the CTL4-6.

Table 1 Optical and electrochemical properties of CTL1-6.

Polymer	λ_{max}^{sol} [nm]	ε^{sol} [cm^{-1} L mol^{-1}]	λ_{max}^{film} [nm]	E_g^{opt} [eV]	E^{ox} [V]	E_{HOMO} [eV]	E^{red} [V]	E_{LUMO} [eV]	E_g^{CV} [eV]
CTL1	430, 642	102200[642 nm]	429, 644	1.75	0.95	-5.75	-1.16	-3.64	2.11
CTL2	431, 643	168300[643 nm]	427, 645	1.75	0.96	-5.76	-1.09	-3.71	2.05
CTL3	428, 635	40300[635 nm]	423, 637	1.78	1.02	-5.82	-1.09	-3.71	2.11
CTL4	425, 631	62700[631 nm]	429, 641	1.75	0.99	-5.79	-1.18	-3.62	2.17
CTL5	422, 629	48500[629 nm]	426, 645	1.75	1.04	-5.84	-1.06	-3.74	2.10
CTL6	426, 627	71200[627 nm]	425, 636	1.80	1.08	-5.88	-1.06	-3.74	2.13

View Article Online
DOI: 10.1039/C7TA09224E

Modifying the experiment from solution to the solid state (Figure S2b), it is demonstrated that the low- and high- wavelength absorption peaks of CTL1-3 do not alter significantly, while for the CTL4-6 a more than 10 nm red shift of the high wavelength absorption maxima is observed without affecting significantly the low wavelength absorption maxima (Table 1). This indicates that the presence of the thiophene rings as substituents on the IDTT seems to assist the effective overlapping between the orbitals of the electron donating and electron withdrawing units passing from solution to the solid state. Moreover, the same trend observed in solution for CTL1-6 regarding the variation of the absorption maxima of both the low- and high- wavelength peaks as a function of the number of fluorine atoms on the BTD is also present in the solid state as well. Furthermore, the optical bandgaps (E_g^{opt}) of CTL1-6 are ranging between 1.75 eV and 1.80 eV. In particular, the E_g^{opt} of CTL2 and CTL4 are 1.75 eV, which are the same with those of CTL1 and CTL3, showing that the addition of one fluorine atom on BTD does not influence the E_g^{opt} of the polymers regardless of the aryl substituent anchored onto the IDTT. However, addition of a second fluorine atom on the BTD (CTL3, CTL6) increases the E_g^{opt} of the polymers. In the case of CTL3 (phenyl substituent) by 0.03 eV (1.78 eV) and for CTL6 (thienyl substituent) by 0.05 eV (1.80 eV). In order to verify if the CTL1-6 exhibit the temperature dependent aggregation property as other fluoro-substituted BTD based polymeric semiconductors,[2a,4a,19] we examined the absorption spectra of CTL1-6 in *o*-DCB solution upon heating up to 95 ^{o}C as shown in Figure 1. It is clearly observed that none of the polymers reveal any temperature-dependent aggregation property but only a blue shift is visible of around 4 to 6 nm of their high wavelength absorption maxima accompanied by a subsequent decrease of their absorption intensity. This points out that the polymer chains of CTL1-6 present tight π-π stacking between the highly fused polycyclic IDTT and strong non-covalent interactions (H···F, S···F, S···N and F···F)[20] among the different building

View Article Online
DOI: 10.1039/C7TA09224E

blocks within the polymer chains even in solution, which prevent them to adopt any coil (extended) conformation at high temperatures (95 ^{o}C).

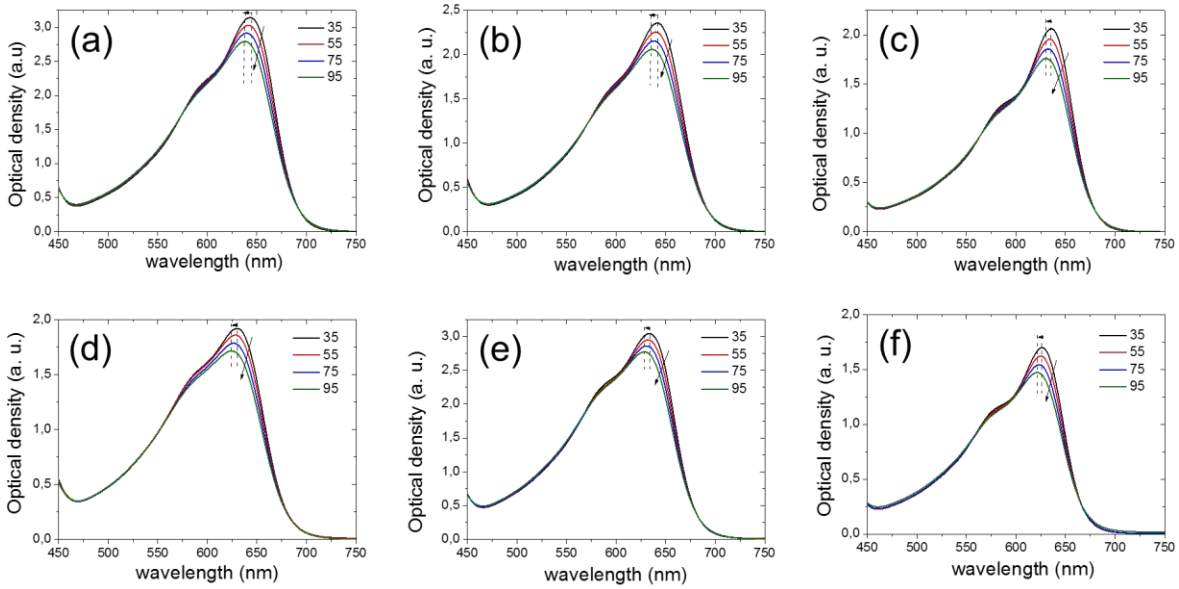

Fig. 1 UV-vis spectra of (a) CTL1, (b) CTL2, (c) CTL3, (d) CTL4, (e) CTL5 and (f) CTL6 in chlorobenzene solution as the temperature increased from 35°C to 95°C. The insets indicate temperatures (units: °C).

In order to estimate the energy levels of the polymers and as a consequence the electrochemical bandgap (E_g^{CV}), cyclic voltammetry (CV) was performed. The oxidation and reduction potentials of CTL1-6 are shown in Figure S3 and the corresponding data along with the lowest unoccupied molecular orbital (E_{LUMO}) and E_{HOMO} energy level values are summarized in Table 1. All the polymers exhibit reversible oxidation and reduction peaks. It is shown that as the number of the fluorine atoms on the BTD increases the E_{HOMO} is downshifted from -5.75 for CTL1 to -5.76 eV for CTL2 and to -5.82 eV for CTL3. In a similar way, the E_{HOMO} is downshifted from -5.79 eV for CTL4 to -5.84 eV for CTL5 and to -5.88 eV for CTL6 as well. On the contrary, while the E_{LUMO} is downshifted from the non-fluorinated derivatives CTL1 (-3.64 eV) and CTL4 (-3.62 eV) to the mono fluorinated derivatives CTL2 (-3.71 eV) and CTL5 (-3.74 eV), the further increase of the

View Article Online
DOI: 10.1039/C7TA09224E

fluorine atoms on the BTD interestingly is not affecting the E_{LUMO} levels of CTL3 (-3.71 eV) and CTL6 (-3.74 eV). Moreover, comparison between the CTL1 and CTL4, CTL2 and CTL5 and CTL3 and CTL6 pairs demonstrates that the polymers containing the thienyl substituents on the IDTT (CTL4-6) present slightly deeper E_{HOMO} and E_{LUMO} levels versus vacuum. This is particularly interesting since that someone would expect the energy levels of CTL4-6 to be upshifted versus vacuum due to the fact of the stronger electron donating property of the thienyl side group as compared to phenyl.[21a] However, the resulting deeper E_{HOMO} and E_{LUMO} levels of CTL4-6 vs CTL1-3 is explained by the σ-inductive effect of thienyl side groups in similar observations with recently reported results on small molecule non fullerene acceptors (NFAs) consisting of phenyl and thienyl substituted IDTT building blocks.[21b] Finally, all the polymers reveal similar E_g^{CV}, which however are significantly increased by ~0.3 to 0.4 eV than their corresponding E_g^{opt} in agreement with recently reported results on other polymer systems.[21c]

2.3 Photovoltaic properties and photophysics

The photovoltaic properties of the polymers:$PC_{71}BM$ systems were investigated by fabricating OPVs in conventional device architecture of ITO/PEDOT:PSS/active layer/Ca/Al. The current density versus voltage (J-V) curves of the devices are presented in Figure 2 and the photovoltaic parameters in Table 2, respectively. Based on the J-V curves of Figure 2a and the OPV results in Table 2, a correlation between IDTT-substituent nature and OPV performance was achieved. Indeed, it is obvious that the polymers with phenyl side groups exhibit superior performances (6.2% for CTL1, 5.3% for CTL2 and 6.1% for CTL3) than those containing the thienyl side groups (2.9% for CTL4, 3.8% for CTL5 and 3.9% for CTL6). However, a general trend correlating the influence of the fluorine atoms on the BTD in CTL1-6 with the PCE and the photovoltaic parameters of the OPV devices cannot be detected, as shown from the results of Table 2. The enhanced PCEs of CTL1-3 as compared to CTL4-6 are mainly attributed to the increased short circuit currents (J_{sc}s),

View Article Online
DOI: 10.1039/C7TA09224E

fill factors (FFs) and external quantum efficiencies (EQEs) (Table 2). However, the physical origin of such a correlation is not straightforward to identify. Previous reports suggested that differences in J_{sc}s, FFs and EQEs may result in either an altered morphological feature, a changed charge transport and/or recombination mechanisms, or in deviating the charge generation rate. To elucidate between these processes a careful study of charge transporting, morphological and photophysical properties was carried out.

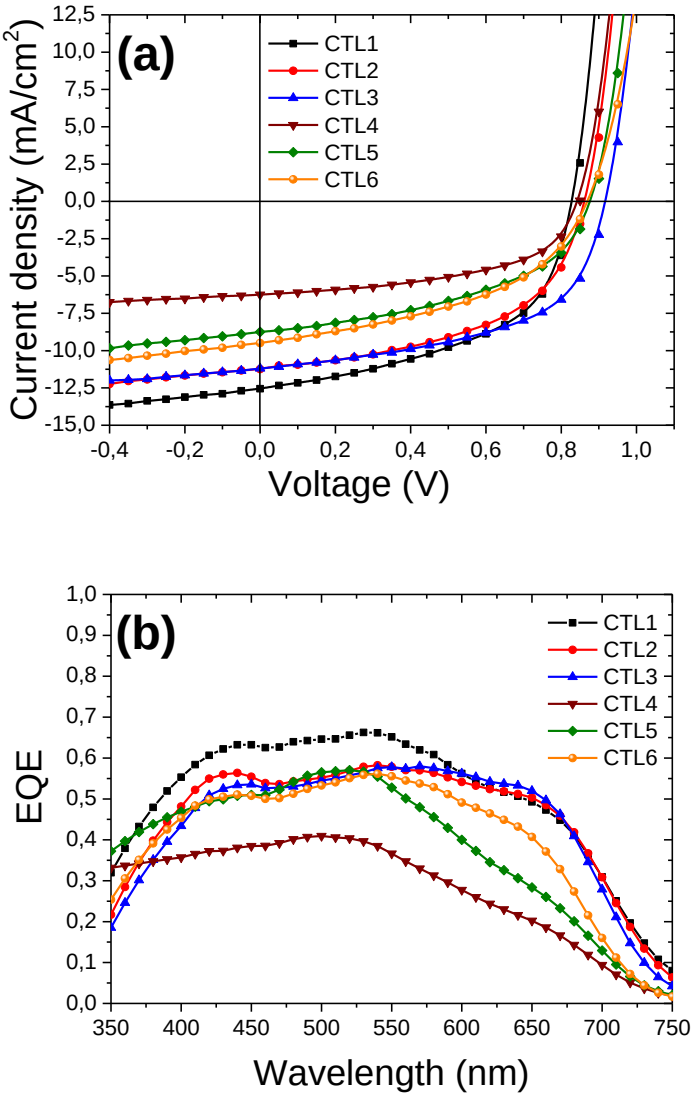

Fig. 2 (a) Current density-Voltage characteristics under standard AM1.5G solar simulator illumination (100 mW/cm^2) and (b) external quantum efficiency (EQE) graphs of CTL1-6:$PC_{71}BM$ conventional organic solar cells.

View Article Online
DOI: 10.1039/C7TA09224E

Table 2 Photovoltaic device parameters of conventional solar cells under standard AM1.5G at 1 sun illumination (100 mW/cm^2) and hole and electrons mobilities based on SCLC model of the polymer:$PC_{71}BM$ systems.

Polymer:$PC_{71}BM$	J_{sc} (mA/cm^2)	V_{oc} (V)	FF	PCE^{aver} (%)	PCE^{max} (%)	μ_h (cm^2/Vs)	μ_e (cm^2/Vs)
CTL1	12.5	0.83	0.55	5.5 ± 0.7	6.2	6.8 x 10^{-3}	6.2 x 10^{-3}
CTL2	11.2	0.87	0.55	4.8 ± 0.8	5.3	6.3 x 10^{-3}	5.8 x 10^{-3}
CTL3	11.2	0.92	0.60	5.7 ± 0.4	6.1	5.6 x 10^{-3}	5.1 x 10^{-3}
CTL4	6.3	0.85	0.54	2.0 ± 0.9	2.9	5.1 x 10^{-3}	3.5 x 10^{-3}
CTL5	8.7	0.87	0.49	3.4 ± 0.4	3.8	3.3 x 10^{-3}	2.1 x 10^{-3}
CTL6	9.5	0.88	0.48	3.4 ± 0.5	3.9	0.3 x 10^{-3}	7.6 x 10^{-3}

We started our analysis by investigating the charge transport properties of the polymer:$PC_{71}BM$ blend films utilizing the space charge limited current (SCLC) model. For each system, unipolar devices were fabricated and their dark J–V characteristics were recorded. The dark J-V curves are presented in Figure S4 in SI. Table 2 summarizes the results of the charge transport characterization of all devices. The obtained hole and electron mobilities values in the order of 10^{-3} cm^2/Vs based on SCLC model are comparable to or greater than those reported for typical high-PCE BHJ films[22a,b] and in agreement to the observed tight π-π stacking and strong non-covalent interactions within the polymer chains (Figure 1; temperature dependent aggregation property section). It is shown that the devices containing CTL1-3 (with phenyl substituents) exhibit in general higher hole and electron mobilities, except in the case of the electron mobility of CTL6, and more balanced as compared to CTL4-6 (containing the thienyl substituents). The more balanced hole and electron mobilities of CTL1-3 may account for their enhanced FFs in agreement with recently reported findings.[22c] Furthermore, a trend in both CTL1-3 and CTL4-6 series could be noticed in which as

View Article Online
DOI: 10.1039/C7TA09224E

the number of fluorine atoms increases on the BTD the hole mobility of the resulting polymer:$PC_{71}BM$ systems decreases.

Then, transmission electron microscopy (TEM) investigations of the active layer films were performed. Figure 3 shows high-resolution (HR) TEM images of the polymer:$PC_{71}BM$ blend films. In general, all the studied systems present finer intermixing of the polymer and the fullerene phases with variable size of the $PC_{71}BM$ aggregates. It is revealed that the size of the $PC_{71}BM$ domains is about 10 to 15 nm in all the systems except in the case of CTL4:$PC_{71}BM$ where the size of the $PC_{71}BM$ aggregates is about 100 nm. This might be an indication for the lower PCE of the CTL4:$PC_{71}BM$ system but the obtained morphological features cannot provide a vibrant explanation for the PCE variation among the other polymer:$PC_{71}BM$ systems and especially the significantly higher PCE of the CTL1-3 against CTL4-6.

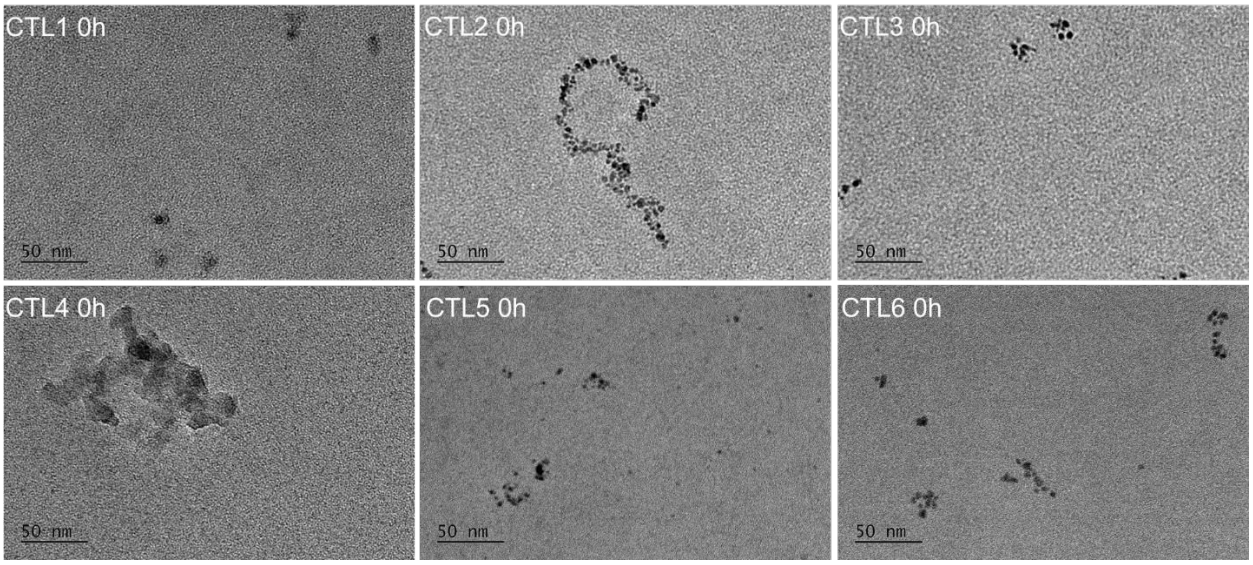

Fig. 3 High resolution transmission electron microscopy (HR-TEM) images of optimized CTL1-6:$PC_{71}BM$ blend films.

For this reason and in order to further explore the influence of the employed polymer semiconductor to the obtained photovoltaic performance (Table 2), solar cell devices were thoroughly investigated by transient absorption spectroscopy (TAS). It is worth mentioning that all

View Article Online
DOI: 10.1039/C7TA09224E

TAS measurements were performed using a specially designed homemade cell enabling us to maintain inert atmospheric conditions throughout the whole measurement duration, i.e. 30 min. Figure 4a and Figure 4b display typical graphs of the relative optical density (ΔOD) versus wavelength at various time delays for samples CTL1 and CTL6, respectively, following photo-excitation at 1026 nm with a pump fluence of 1.5 mJ/cm^2. The main ΔOD peak at ca. 650 nm is attributed to the transient photo-induced bleaching of the band edge transition, while a photo-induced transient absorption (PIA) in the range of 700-900 nm is also observed and found to notably attenuate with time.

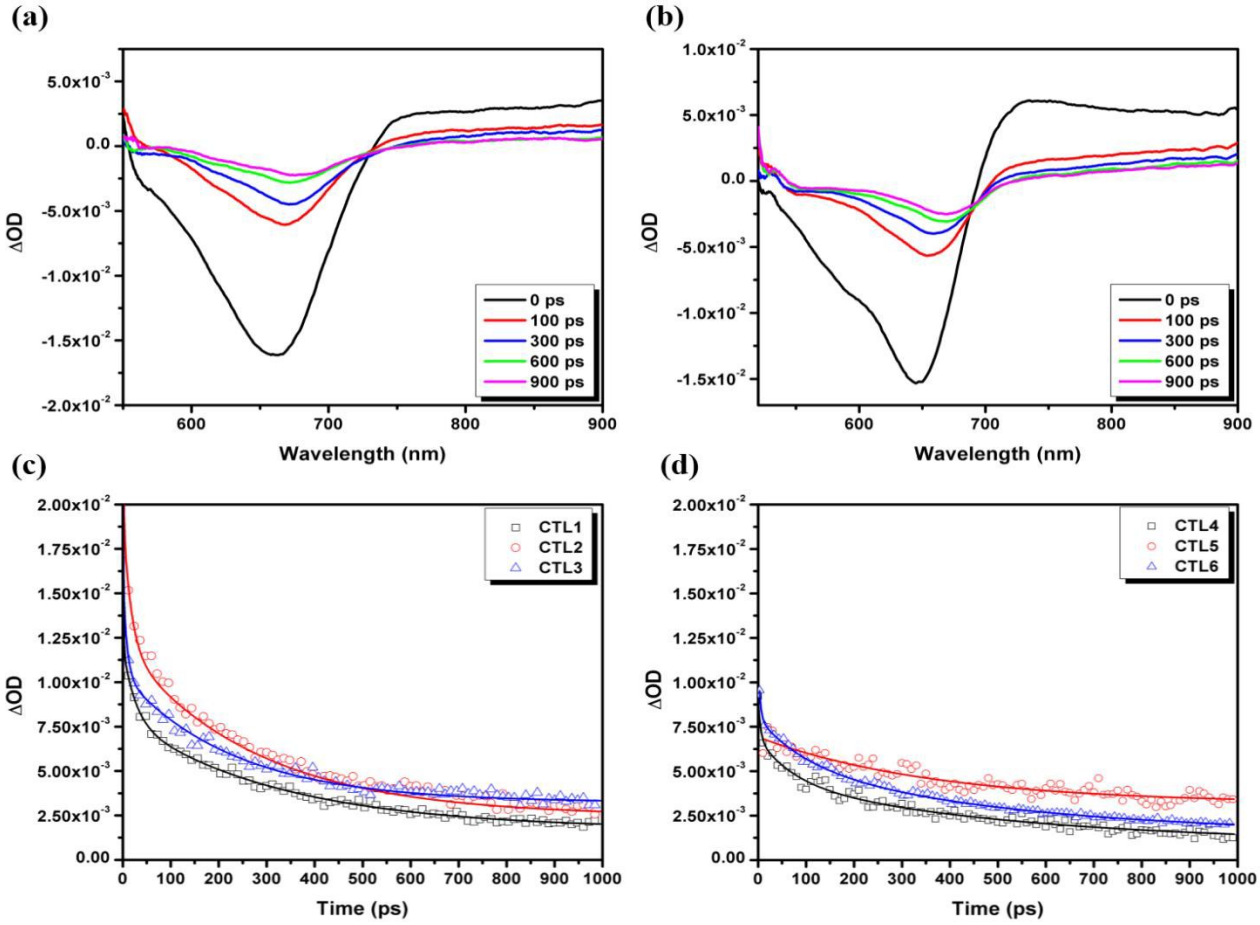

Fig. 4 Typical transient absorption spectroscopy (TAS) of corresponding ΔOD vs. wavelength plots at various time delays following photoexcitation at 1026 nm with a pump fluence of 1.5 mJ/cm^2 for CTL1 (a) and CTL6 (b); Transient band edge bleach kinetics (symbols) and their corresponding decay exponential fits (lines) for Glass/ITO/PEDOT:PSS/CTL1-3:$PC_{71}BM$ (c) and Glass/ITO/PEDOT:PSS/CTL4-6:$PC_{71}BM$ (d) configurations. For the sake of comparison, same y-axis scales were employed for the latter two graphs.

View Article Online
DOI: 10.1039/C7TA09224E

The relaxation dynamics of the transient photo-induced bleaching and the corresponding decay kinetics were determined following exponential fittings, as presented in Figure 4c and Figure 4d for samples CTL1-3 and CTL4-6, respectively. For this purpose, a biexponential third order equation of the form $y = y_0 + A_1\exp(-x/\tau_1) + A_2\exp(-x/\tau_2) + A_3\exp(-x/\tau_3)$ was employed to fit the summary of excited state decay kinetics, i.e. ΔOD versus time. The obtained kinetic fit parameters for all architectures are summarized in Table 3, while all employed adjusted r squared (R^2) interpretation values were above 0.995, indicative of excellent quality fittings.

Table 3. Kinetic fit parameters for Glass/ITO/CTL-$PC_{71}BM$ architectures.

	λ_{max} (nm)	τ_1 (ps)	τ_2 (ps)	τ_3 (ps)
CTL1	677	0.80	12	260
CTL2	666	1.00	16	286
CTL3	655	0.80	8	240
CTL4	657	2.00	50	428
CTL5	665	1.00	25	390
CTL6	643	0.80	20	287

It is important to have in mind the key photophysical processes occurring when a photon is absorbed within the active layer of an organic solar cell: (i) photon absorption generates an excited state, namely a Coulombically bound exciton, on the donor (acceptor) material and (ii) this exciton typically undergoes ultrafast charge transfer at the donor–acceptor interface where an energetic driving force assists the transfer of an electron (hole) from the donor (acceptor) to the acceptor (donor), while often a small fraction of the initial exciton population also shows diffusion-limited dissociation. Although it is not yet completely clear how the free carriers are formed,[23-27] the result is a spatially separated electron-hole pair. Our understanding of this charge transfer process is that within a short time typically within several picoseconds either free charges (potentially through a very short-lived delocalized intermediate) or a bound charge-transfer (CT) state at the interface is

View Article Online
DOI: 10.1039/C7TA09224E

formed upon charge transfer. The splitting ratio between these two populations depends on material and morphology.[25] Subsequently, free charges can nongeminately recombine or be extracted from the device, while the initial CT-state population decays monomolecularly. Nongeminate recombination is frequently termed "bimolecular recombination"; however, the reaction order for this process has in several material systems been found to be greater than 2 and in many cases approaching 3, on account of the density dependence of charge carrier mobility within an energetically disordered system,[28,29] and furthermore upon the geometric restrictions at the polymer:fullerene interface.[25]

Inspection of Table 3 reveals that the first time component (τ_1) varies slightly from 0.8 to 2 ps for all devices in question. Namely, (τ_1) corresponds to exciton dissociation that is found to be an ultrafast process for all samples,[30,31] and thus, has indistinguishable effect on the electrical characteristics of the devices (Table 2). More interestingly, the second time component (τ_2) is attributed to the free electron-hole charge carriers transfer from the active layer to the hole transport layer (HTL) of the device,[30-34] i.e. PEDOT:PSS in this case. This process is considered to play a major role on the device performance and electrical characteristics. Remarkably, τ_2 is found to be noticeably smaller for samples CTL1-3 than those of CTL4-6, suggesting considerably faster free electron-hole charge carriers transfer processes when phenyl groups are used as substituents in the polymer backbone of CTLs. Indicatively, the device consisting of the phenyl substituent polymer CTL3 exhibits a τ_2 component of 8 ps, which is 2.5 times faster as compared to the corresponding time of 20 ps for the faster thienyl substituted polymer CTL6. These findings are in agreement with a study by *Guo et al.*[34] in which faster hole extraction rates are also reported for the devices with enhanced PCE.

Furthermore, Table 3 includes the third long-life time component (τ_3), which is representative of the free electron-hole charge carriers recombination rate following excitation.[35-37] In principle,

View Article Online
DOI: 10.1039/C7TA09224E

longer free electron-hole charge carriers lifetimes are beneficial for the electrical performance of the devices as it reduces the propagation for charge carrier recombination and enables the efficient collection of the free charge carriers to the selective electrodes. Interestingly enough, Table 3 reveals higher τ_3 times for the CTL4-6 solar cell devices as compared to the corresponding times of CTL1-3, indicative of prolonged free electron-hole charge carriers lifetimes when thienyl substituents are anchored onto the polymer backbone. However, as stated earlier, the solar cell devices consisting of the CTL1-3 (phenyl substituents) exhibit significantly higher electrical performances (Table 2). Such findings suggest further that the critical time component and process for the enhanced J_{sc} values exhibited by CTL1-3 based-devices is the fast and efficient free charge carriers extraction to the transport layers, i.e. as depicted by the second time component τ_2. In the case of solar cell devices with CTL4-6 (thienyl substituents), even though that free electron-hole charge carriers with longer lifetimes are formed, the slow extraction process at the interface with the transport layers of the devices limits the J_{sc} values.

2.4 Photovoltaic stability

Research into OPV materials has recently been focused also on improving the photostability of semiconducting polymers. Usually the degradation observed in OPVs falls into three general time regimes: an initial period of photoinduced degradation that slows down with time, a period of relatively constant degradation that lasts for most of the solar cell's usable lifetime, and rapid and complete degradation that results in device failure.[5] The initial period of photoinduced degradation the so called "burn-in" exhibits the shape of exponential decay of efficiency. It is remarkable that this photo-induced burn-in ends without completely degrading the solar cell's efficiency, and several competing hypotheses attempt to account for both the kinetics of burn-in and why it stops. It has been suggested that potential origins, include oxygen trapped within the films, the broad

View Article Online
DOI: 10.1039/C7TA09224E

dispersity of the polymer samples, and organic or inorganic impurities in the polymers (such as palladium catalysts, tin- or halogen-containing molecules, unreacted monomer moieties, cross-coupling byproducts within the polymer samples and so on),[38] however photo-dimerization of the $PC_{61}BM$ has been proven so far to be a key mechanism for the burn-in that leads to J_{sc} loss.[5,12b,39] However, up to now a systematic study on the role of the conjugated polymer's chemical features on the burn-in effect is still missing. To address this concern, we examined the photo-stability of our synthesized polymers by placing the as fabricated devices under in a sealed, electronically controlled degradation chamber with regulated environment (O_2 < 1ppm, H_2O < 1ppm). The J-V characteristics of the organic solar cells were probed periodically while continuously light-soaked using white light LEDs irradiating at 100 mW/cm^2.[40] The PCEs and individually the photovoltaic parameters of each OPV device versus the photo-degradation process are presented in Figure 5.

At least after the first 48 h of illumination, the burn-in effect still occurs to all the studied OPV devices. It is obvious though that its kinetic is dependent on the choice of the electron donor polymer in the active layer of the devices. In particular, a clear trend is detected. CTL3 and CTL6 with the two fluorine atoms on the BTD demonstrate better resistivity to photo-degradation process, with CTL3 being slightly enhanced as compared to CTL6. Among CTL1-3, CTL1 (no fluorine atom on BTD) and CTL2 (one fluorine atom on BTD) exhibit similar degradation kinetics, whereas among CTL4-6 the degradation rate (burn-in kinetics) and the period of relatively constant degradation follows this order: CTL4 (no fluorine atom on BTD) > CTL5 (one fluorine atom on BTD) > CTL6 (two fluorine atoms on BTD). Between the CTLs with the different aryl substituents, no significant variation can be detected, with CTL1-3 containing the phenyl substituents on the IDTT slightly slows down the burn-in and consequently enhance the overall stability of the OPV devices than CTL4-6 (thienyl substituents on the IDTT). However, someone should take into account that the variation on the $\overline{M_n}$ among the pairs of CTLs possessing the different aryl groups

View Article Online
DOI: 10.1039/C7TA09224E

(CTL1 versus CTL4, CTL2 versus CTL5 and CTL3 versus CTL6) could also contribute to the observed differences on the photo-degradation. Nevertheless, after 470 h light exposure to OPV devices, the PCEs of CTL1, CTL2, and CTL3 decreased by 31, 32, and 20% of the initial PCEs, respectively whereas those of CTL4-6 by 45% (CTL4), 35% (CTL5) and 20% (CTL6), of the initial PCEs.

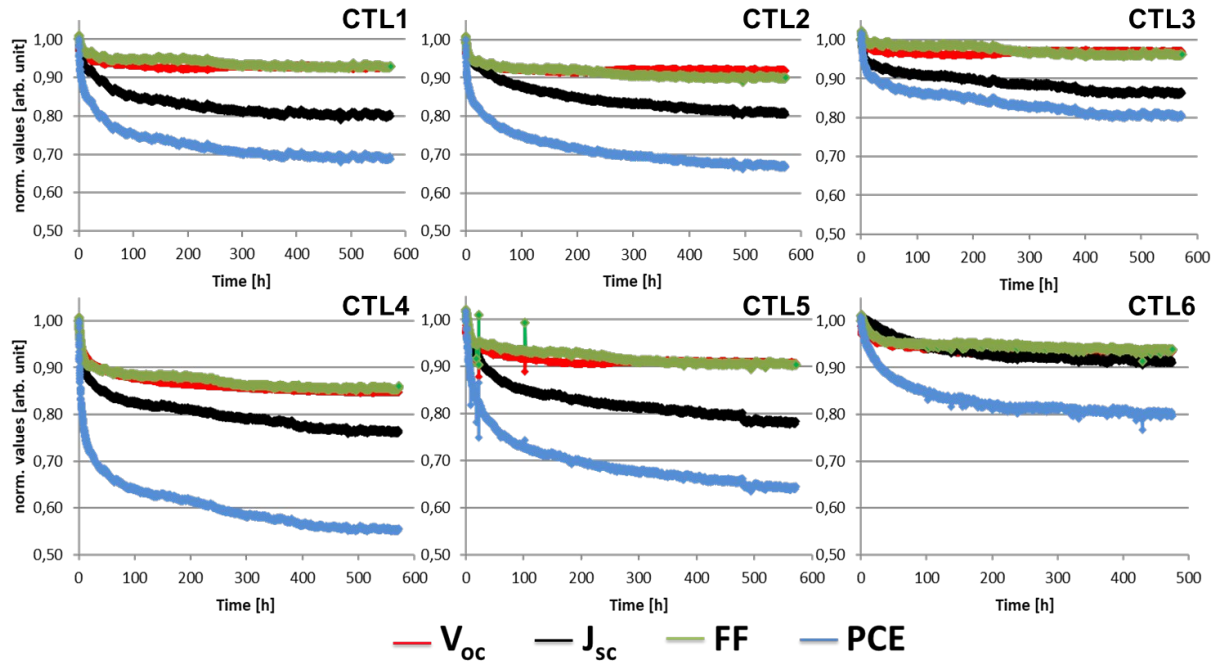

Fig. 5 Photo-stability of polymer:$PC_{71}BM$ solar cells (in air, un-encapsulated, under AM1.5 illumination at 1 sun).

In order to provide further insights on the origin of the burn-in and the photo-degradation properties of the OPV devices upon light exposure, the UV-vis absorption spectra of CTL1-6:$PC_{71}BM$ blend films as a function of photo-degradation time under 1 sunlight illumination in nitrogen atmosphere for the first 48 h, which corresponds to the time scale where the burn-in effect still occurs, were recorded and presented in Figure S5. The results demonstrate that the absorption spectra before

View Article Online
DOI: 10.1039/C7TA09224E

and after photo-degradation are almost identical. This indicates that CTL polymers are stable to photo-oxidation due to the synergistic occurrences of oxygen absence during the light exposure, stabilizing effect of the PCBM[41] and the tight π-π stacking and strong non-covalent interactions behavior of the polymer chains in accordance to recent findings on similar polycyclic (ladder-type) conjugated polymers with planar backbone polymer chains.[42] To confirm further the chemical integrity of the active layer components towards photo-oxidation micro-Raman spectroscopy studies were performed. All the spectral features of the original molecular vibrations in the polymer films were preserved, even after a 48 h sunlight exposure (Figure S6). These results point out that the observed variations on the stability of the OPV devices cannot be attributed to any chemical changes induced during light exposure.

By studying further the impact of the photo-oxidation on the individual photovoltaic parameters, a very interesting trend on the amount of J_{sc} loss during the burn-in effect has been observed on the OPV devices (Figure 5). The polymers with the two fluorine atoms on the BTD (CTL3, CTL6) present enhanced long term photo-stability and reduced J_{sc} loss during the burn-in as compared to the monofluoro polymers (CTL2, CTL5) and nonfluorinated polymers (CTL1, CTL4). The fact that in this study $PC_{71}BM$ was employed as the electron acceptor material minimize the impact of the dimerization of the fullerene derivative as the primary factor for the observed J_{sc} loss and PCE variation during the photo-oxidation since dimerization of $PC_{71}BM$ is known to be very weak.[43] Therefore, in order to provide more insights about the different burn-in behavior of the examined polymer:$PC_{71}BM$ systems, morphological studies on the photo-oxidative active layer components after 48h of exposure have been performed by HR-TEM (Figure 6).

View Article Online
DOI: 10.1039/C7TA09224E

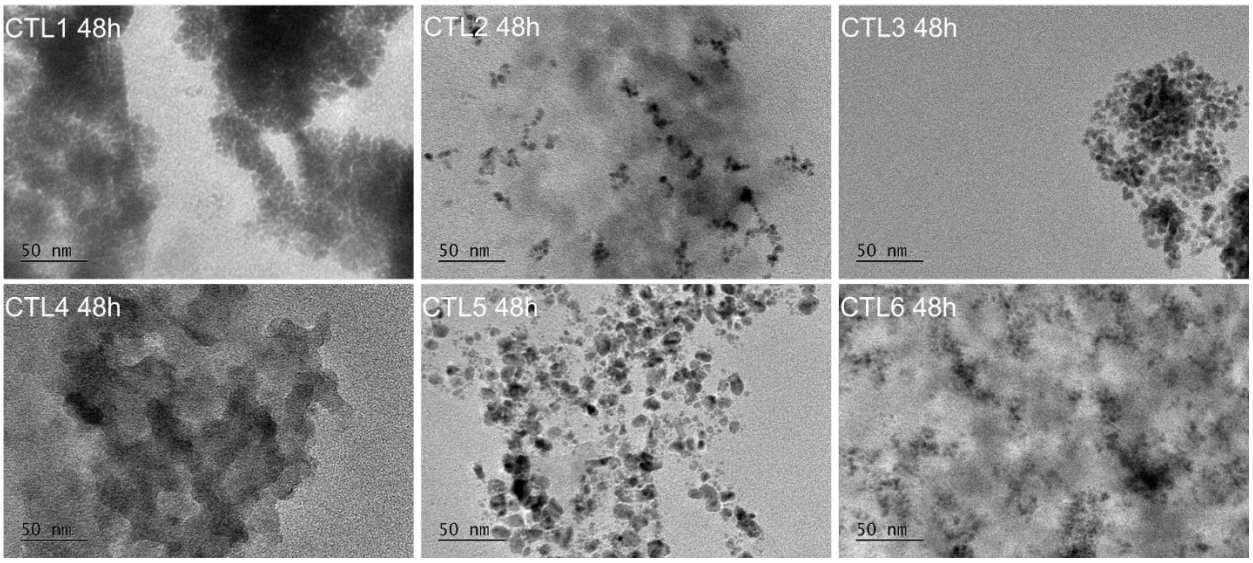

Fig. 6 High resolution transmission electron microscopy (HR-TEM) images of photo-oxidative CTL1-6:$PC_{71}BM$ blend films after 48h.

By comparing the morphology of the unexposed polymer:$PC_{71}BM$ systems (0h; Figure 3) with the morphology of the polymer:$PC_{71}BM$ systems after 48h of exposure (Figure 6) a clear alteration of the microstructure is observed. It is therefore evident that the observed burn-in effect in the examined polymer:$PC_{71}BM$ systems can be attributed to the microstructure alteration during photo-oxidation in accordance with some recent findings.[44] Furthermore, the presence of the two fluorine atoms on the BTD in CTL3 and CTL6 must enable tighter π-π stacking and stronger non-covalent attractive intra/inter-chain interactions versus the nonfluorinated and monofluorinated derivatives (CTL1, CTL2, CTL4 and CTL5) that is known to result in quite close π-π polymer chain stacking.[16,20] Therefore, we believe that the beneficial effect of the closer π-π polymer chains stacking in CTL3 and CTL6 probably slows down the diffusion of the $PC_{71}BM$ from the bulk resulting to reduce phase separation. This is more evident if someone compares CTL1 with CTL3 and CTL4 with CTL6 which strong $PC_{71}BM$ aggregation occurs with the appearance of severe phase separation for the nonfluorinated derivatives CTL1, CTL4 versus the difluoro derivatives CTL3, CTL6 (Figure 6).

View Article Online
DOI: 10.1039/C7TA09224E

3. Conclusions

In conclusion, a series of D-A conjugated polymers based on IDTT as the electron donating unit and BTD as the electron withdrawing moiety have been successfully synthesized containing various aryl substituents and number of fluorine atoms. A correlation between polymer chemical structure – optoelectronic properties – organic solar cell performance and stability relationship in this series of D-A copolymers was achieved. In particular, both CTL1-3 and CTL4-6 exhibit similar absorption maxima in the solid state and E_g^{opt} between 1.75 eV to 1.80 eV dependent on the number of the fluorine atoms on the BTD. In addition, the presence of two fluorine atoms on BTD results to the blue shift of the high wavelength absorption maxima as compared to the monofluoro and non-fluorinated analogues, without affecting significantly the low wavelength absorption maxima. It is also interesting to note that none of the polymers reveal any temperature-dependent aggregation property. Moreover, both the E_{HOMO} and E_{LUMO} are downshifted as the number of the fluorine atoms on the BTD increases, except in the cases of CTL3 and CTL6 where the presence of two fluorine atoms on the BTD does not alter the E_{LUMO} as compared to the monofluoro derivatives. Again, it should be pointed out that the polymers containing the thienyl substituents on the IDTT (CTL4-6) present slightly deeper E_{HOMO} and E_{LUMO} levels.

From the studies of their OPV performances, it is obvious that the polymers with phenyl substituents exhibit superior efficiencies than those containing the thienyl side groups in all cases. However, a general trend correlating the influence of the fluorine atoms on the BTD with the PCE and the photovoltaic parameters of the OPV devices cannot be detected. The enhanced PCEs of CTL1-3 as compared to CTL4-6 are mainly attributed to the increased short circuit currents (J_{sc}s), fill factors (FFs) and external quantum efficiencies (EQEs) due to the synergistic effects of higher

View Article Online
DOI: 10.1039/C7TA09224E

and balanced hole and electron mobilities and faster free electron-hole charge carrier transfer process from the active layer to the HTL of the device.

Finally, one of the most important findings is that polymer solar cells with significantly improved lifetime, in which an initial burn-in loss is substantially reduced through the rational design of the polymeric semiconductor's chemical structure, are demonstrated. The 20% initial PCE loss after almost 500h of photo-oxidation for the CTL3 and CTL6 systems are one of the lowest reported values for polymer:fullerene bulk heterojunction (BHJ) solar cells. Since that the dimerization of $PC_{71}BM$ is known to be very weak, we can safely attribute that the primary factor for the significant variation of the burn-in observed in these studies do come from microstructure instabilities as evidenced by HR-TEM studies. Moreover, we identify the beneficial effect of the presence of the two fluorine atoms on the BTD, as compared to the non-fluorinated and mono-fluorinated analogues, in suppressing the burn-in by reducing the microstructure instabilities regardless of the aryl substituent that is present in the polymer backbone. We envision these insights will guide the synthetic chemists and materials scientists towards the optimization of polymer chemical structures with predetermined optoelectronic properties towards organic solar cells that will demonstrate simultaneously high PCEs and stabilities. Further studies including the grazing-incidence wide-angle X-ray scattering (GIWAXS) as well as replacement of the $PC_{71}BM$ with non-fullerene acceptors (NFA) are in progress for the complete analysis of the self assemby behavior of the polymer chains in the blend and the further enhacement of the PCE.

4. Experimental

All experimental and instrumental details, including synthesis, gel permeation chromatography, absorption spectroscopy and cyclic voltammetry characterisation of the polymers along with the

View Article Online
DOI: 10.1039/C7TA09224E

fabrication and characterisation of organic solar cells, transport characteristics and transient absorption spectroscopy of the devices and finally high resolution transmission electron microscopy and micro-RAMAN spectroscopy are given in the ESI.†

Conflicts of interest

There are no conflicts to declare.

Acknowledgment

This project has received funding from the European Community's Seventh Framework Programme (FP7/2007-2013) under the Grant Agreements n° 331389 project ECOCHEM, n° 607585 project OSNIRO and nº 604603 project MatHero. CLC, ET, AK, DM and AA would like to acknowledge the Network of Research Supporting Laboratories at the University of Ioannina for using the Electron Microscopy Facility.

References

1. a) C. L. Chochos and S. A. Choulis, *Prog. Polym. Sci.*, 2011, **36**, 1326; b) G. Dennler, M. C. Scharber and C. J. Brabec, *Adv. Mater.*, 2009, **21**, 1323; c) A. J. Heeger, *Adv. Mater.*, 2014, **26**, 10; d) L. Dou, J. You, Z. Hong, Z. Xu, G. Li, R. A. Street and Y. Yang, *Adv. Mater.*, 2013, **25**, 6642; e) X. Guo, M. Baumgarten and K. Müllen, *Prog. Polym. Sci.*, 2013, **38**, 1832; f) X. Guo, A. Facchetti and T. J. Marks, *Chem. Rev.*, 2014, **114**, 8943; g) H. Yao, L. Ye, H. Zhang, S. Li, S. Zhang and J. Hou, *Chem. Rev.*, 2016, **116**, 739; h) Y.-J Cheng, S.-H. Yang and C.-S. Hsu, *Chem. Rev.*, 2009, **109**, 5868.

View Article Online
DOI: 10.1039/C7TA09224E

2. a) J. Zhao, Y. Li, G. Yang, K. Jiang, H. Lin, H. Ade, W. Ma and H. Yan, *Nat. Energy*, 2016, **1**, 15027; b) S. Li, L. Ye, W. Zhao, S. Zhang, S. Mukherjee, H. Ade and J. Hou, *Adv. Mater.*, 2016, **28**, 9423.

3. a) X. Wang, C. X. Zhao, G. Xu, Z.-K. Chen and F. Zhu, *Sol. Energy Mater. Sol. Cells*, 2012, **104**, 1; b) G. Williams and H. Aziz, *Org. Electron.*, 2014, **15**, 47.

4. a) Y. Liu, J. Zhao, Z. Li, C. Mu, W. Ma, H. Hu, K. Jiang, H. Lin, H. Ade and H. Yan, *Nat. Commun.*, 2014, **5**, 5293; b) W. Li, B. Guo, C. Chang, X. Guo, M. Zhang and Y. Li, *J. Mater. Chem. A*, 2016, **4**, 10135; c) J. Subbiah, B. Purushothaman, M. Chen, T. Qin, M. Gao, D. Vak, F. H. Scholes, X. Chen, S. E. Watkins, G. J. Wilson, A. B. Holmes, W. W. H. Wong and D. J. Jones, *Adv. Mater*., 2015, **27**, 702; d) N. Wang, W. Chen, W. Shen, L. Duan, M. Qiu, J. Wang, C. Yang, Z. Dua and R. Yang, *J. Mater. Chem. A*, 2016, **4**, 10212; e) L. Huo, T. Liu, B. Fan, Z. Zhao, X. Sun, D. Wei, M. Yu, Y. Liu and Y. Sun, *Adv. Mater.*, 2015, **27**, 6969; f) M. Zhang, X. Guo, W. Ma, H. Ade and J. Hou, *Adv. Mater.*, 2015, **27**, 4655; g) L. Huo, T. Liu, X. Sun, Y. Cai, A. J. Heeger and Y. Sun, *Adv. Mater.*, 2015, **27**, 2938; h) K. Kawashima, Y. Tamai, H. Ohkita, I. Osaka and K. Takimiya, *Nat. Commun.*, 2015, **6**, 10085; i) V. Vohra, K. Kawashima, T. Kakara, T. Koganezawa, I. Osaka, K. Takimiya and H. Murata, *Nat. Photon.*, 2015 **9**, 403; j) W. Yue, R. S. Ashraf, C. B. Nielsen, E. C.-Fregoso, M. R. Niazi, S. A. Yousaf, M. Kirkus, H.-Y. Chen, A. Amassian, J. R. Durrant and I. McCulloch, *Adv. Mater.*, 2015, **27**, 4702; k) J.-H. Kim, J. B. Park, I. H. Jung, A. C. Grimsdale, S. C. Yoon, H. Yang and D.-H. Hwang, *Energy Environ. Sci*., 2015, **8**, 2352; l) H. Choi, S.-J. Ko, T. Kim, P.-O. Morin, B. Walker, B. H. Lee, M. Leclerc, J. Y. Kim and A. J. Heeger, *Adv. Mater.*, 2015, **27**, 3318.

5. a) M. Jørgensen, K. Norrman, S. A. Gevorgyan, T. Tromholt, B. Andreasen and F. C. Krebs, *Adv. Mater.*, 2012, **24**, 580; b) W. R. Mateker and M. D. McGehee, *Adv. Mater.*, 2017, **29**, 1603940; c) I. F. Domínguez, A. Distler and L. Lüer, *Adv. Energy Mater*., 2016, **6**, 1601320; d) Q.

View Article Online
DOI: 10.1039/C7TA09224E

Liu, J. Toudert, F. Liu, P. Mantilla-Perez, M. M. Bajo, T. P. Russell and J. Martore, *Adv. Energy Mat.*, 2017, 1701201; e) M. B. Upama, M. Wright, B. Puthen-Veettil, N. K. Elumalai, M. A. Mahmud, D. Wang, K. H. Chan, C. Xu, F. Haquea and A. Uddin, *RSC Adv.*, 2016, **6**, 103899.

6. a) C. H. Peters, I. T. Sachs-Quintana, J. P. Kastrop, S. Beaupre, M. Leclerc and M. D. McGehee, *Adv. Energy Mater.*, 2011, **1**, 491; b) J. E. Carle, M. Helgesen, M. V. Madsen, E. Bundgaard and F. C. Krebs, *J. Mater. Chem. C*, 2014, **2**, 12901297; c) M. Hosel, R. R. Sondergaard, M. Jorgensen and F. C. Krebs, *Adv. Eng. Mater.*, 2013, **15**, 1068; d) J. M. Kroon, M. M. Wienk, W. J. H. Verhees and J. C. Hummelen, *Thin Solid Films*, 2002, **403-404**, 223; e) G. Dennler, C. Lungenschmied, H. Neugebauer, N. S. Sariciftci, M. Latreche, G. Czeremuszkin and M. R. Wertheimer, *Thin Solid Films*, 2006, **511-512**, 349; f) N. Kim and S. Graham, *Thin Solid Films*, 2013, **547**, 57; g) R. Roesch, K.-R. Eberhardt, S. Engmann, G. Gobsch and H. Hoppe, *Sol. Energy Mater. Sol. Cells*, 2013, **117**, 59; h) R. Tipnis, J. Bernkopf, S. Jia, J. Krieg, S. Li, M. Storch and D. Laird, *Sol. Energy Mater. Sol. Cells*, 2009, **93**, 442; i) S. B. Sapkota, A. Spies, B. Zimmermann, I. Durr and U. Wurfel, *Sol. Energy Mater. Sol. Cells*, 2014, **130**, 144.

7. a) S. Chambon, A. Rivaton, J.-L. Gardette, M. Firon and L. Lutzen, *J. Polym. Sci., Part A: Polym. Chem.*, 2007, **45**, 317; b) S. Chambon, A. Rivaton, J.-L. Gradette and M. Firon, *J. Polym. Sci., Part A: Polym. Chem.*, 2009, **47**, 6044; c) A. Rivaton, S. Chambon, M. Manceau, J.-L. Gardette, N. Lemaître and S. Guillerez, *Polym. Degrad. Stab.*, 2010, **95**, 278; d) S. Chambon, A. Rivaton, J.-L. Gardette and M. Firon, *Polym. Degrad. Stab.*, 2011, **96**, 1149.

8. a) M. Leclerc, *J. Polym. Sci. Part A: Polym. Chem.*, 2001**, 39**, 2867; b) D. Neher, *Macromol. Rapid. Commun.*, 2001, **22**, 1365; c) U. Scherf and E. J. W. List, *Adv. Mater.*, 2002, **14**, 477; d) C. L. Chochos, P. K. Tsolakis, V. G. Gregoriou and J. K. Kallitsis, *Macromolecules*, 2004, **37**, 2502; e) C. L. Chochos, J. K. Kallitsis and V. G. Gregoriou, *J. Phys. Chem. B*, 2005, **109**, 8755; f) R. Grisorio, G. Allegretta, P. Mastrorilli and G. P. Suranna, *Macromolecules*, 2011, **44**, 7977.

View Article Online
DOI: 10.1039/C7TA09224E

9. a) M. Manceau, S. Chambon, A. Rivaton, J.-L. Gardette, S. Guillerez and N. Lemaître, *Sol. Energy Mater. Sol. Cells*, 2010, **94**, 1572; b) H. Hintz, H.-J. Egelhaaf, H. Peisert and T. Chassé, *Polym. Degrad. Stab.*, 2010, **95**, 818; c) M. Manceau, A. Rivaton, J.-L. Gardette, S. Guillerez and N. Lemaître, *Polym. Degrad. Stab.*, 2009, **94**, 898; d) D. E. Motaung, G. F. Malgas and C. J. Arendse, *J. Mater. Sci.*, 2011, **46**, 4942; e) C. J. Brabec, G. Zerza, G. Cerullo, S. De Silvestri, S. Luzzati, J. C. Hummelen and S. Sariciftci, *Chem. Phys. Lett.*, 2001, **340**, 232; f) M. O. Reese, A. M. Nardes, B. L. Rupert, R. E. Larsen, D. C. Olson, M. T. Lloyd, S. E. Shaheen, D. S. Ginley, G. Rumbles and N. Kopidakis, *Adv. Funct. Mater.*, 2010, **20**, 3476; g) J. Schafferhans, A. Baumann, A. Wagenpfahl, C. Deibel and V. Dyakonov, *Org. Electron.*, 2010, **11**, 1693; h) A. Seemann, H.-J. Egelhaaf, C. J. Brabec and J. A. Hauch, *Org. Electron.*, 2010, **10**, 1424; i) A. Aguirre, S. C. J. Meskers, R. A. J. Janssen and H.-J. Egelhaaf, *Org. Electron.*, 2011, **12**, 1657; j) A. Seemann, T. Sauermann, C. Lungenschmied, O. Armbruster, S. Bauer, H.-J. Egelhaaf and J. Hauch, *Sol. Energy*, 2011, **85**, 1238; k) J. Abad, A. Urbina and J. Colchero, *Org. Electron.*, 2011, **12**, 1389; l) J. Abad, N. Espinosa, R. Garcia-Valverde, J. Colhero and A. Urbina, *Sol. Energy Mater. Sol. Cells*, 2011, **95**, 1326.

10. a) F. C. Krebs, T. Tromholt and M. Jørgensen, *Nanoscale*, 2010, **2**, 873; b) G. D. Spyropoulos, P. Kubis, N. Li, D. Baran, L. Lucera, M. Salvador, T. Ameri, M. M. Voigt, F. C. Krebs and C. J. Brabec, *Energy Environ. Sci.*, 2014, **7**, 3284.

11. a) M. Manceau, E. Bundgaard, J. E. Carle, O. Hagemann, M. Helgesen, R. Sondergaard, M. Jorgensen and F. C. Krebs, *J. Mater. Chem.*, 2011, **21**, 4132; b) W. R. Mateker, T. Heumueller, R. Cheacharoen, I. T. Sachs-Quintana, M. D. McGehee, J. Warnan, P. M. Beaujuge, X. Liu and G. C. Bazan, *Chem. Mater.*, 2015, **27**, 6345; c) Y. W. Soon, S. Shoaee R. S. Ashraf, H. Bronstein, B. C. Schroeder, W. Zhang, Z. Fei, M. Heeney, I. McCulloch and J. R. Durrant, *Adv. Funct. Mater.*, 2014,

View Article Online
DOI: 10.1039/C7TA09224E

24, 1474; d) Y. Kim and T. M. Swager, *Chem. Commun.* **2005**, 372; e) S. Subramanian, S. K. Park, S. R. Parkin, V. Podzorov, T. N. Jackson and J. E. Anthony, *J. Am. Chem. Soc.*, 2008, **130**, 2706.

12. a) J. Kong, S. Song, M. Yoo, G. Y. Lee, O. Kwon, J. K. Park, H. Back, G. Kim, S. H. Lee, H. Suh and K. Lee, *Nat. Commun.*, 2014, **5**, 5688; b) T. Heumueller, W. R. Mateker, A. Distler, U. F. Fritze, R. Cheacharoen, W. H. Nguyen, M. Biele, M. Salvador, M. von Delius, H.-J. Egelhaaf, M. D. McGehee and C. J. Brabec, *Energy Environ. Sci.*, 2015, **9**, 247; c) C. H. Peters, I. T. Sachs-Quintana, W. R. Mateker, T. Heumueller, J. Rivnay, R. Noriega, Z. M. Beiley, E. T. Hoke, A. Salleo and M. D. McGehee, *Adv. Mater.*, 2012, **24**, 663.

13. a) E. S. R. Bovill, J. Griffin, T. Wang, J. W. Kingsley, H. Yi, A. Iraqi, A. R. Buckley and D. G. Lidzey, *Appl. Phys. Lett.*, 2013, **102**, 183303; b) E. Voroshazi, I. Cardinaletti, T. Conard and B. P. Rand, *Adv. Energy Mater.*, 2014, **4**, 1400848; c) T. M. Clarke, C. Lungenschmied, J. Peet, N. Drolet, K. Sunahara, A. Furube and A. J. Mozer, *Adv. Energy Mater.*, 2013, **3**, 1473; d) Q. Burlingame, X. Tong, J. Hankett, M. Slootsky and S. R. Forrest, *Energy Environ. Sci.*, 2015, **8**, 1005; e) D. Gedefaw, M. Tessarolo, M. Prosa, M. Bolognesi, P. Henriksson, W. Zhuang, M. Seri, M. Muccini and M. R. Andersson, *Sol. Energy Mater. Sol. Cells*, 2016, **144**, 150.

14. a) Y.-X. Xu, C.-C. Chueh, H.-L. Yip, F.-Z. Ding, Y.-X. Li, C.-Z. Li, X. Li, W.-C. Chen and A. K.-Y. Jen, *Adv. Mater.*, 2012, **24**, 6356; b) K. Yao, M. Salvador, C.-C. Chueh, X.-K. Xin, Y.-X. Xu, D. W. deQuilettes, T. Hu, Y. Chen, D. S. Ginger and A. K.-Y. Jen, *Adv. Energy Mater.*, 2014, **4**, 1400206; c) X. Xu, Z. Li, O. Bäcke, K. Bini, D. I. James, E. Olsson, M. R. Andersson and E. Wang, *J. Mater. Chem. A*, 2014, **2**, 18988; d) N. Gasparini, A. Katsouras, M. I. Prodromidis, A. Avgeropoulos, D. Baran, M. Salvador, S. Fladischer, E. Spiecker, C. L. Chochos, T. Ameri and C. J. Brabec, *Adv. Funct. Mater.*, 2015, **25**, 4898; e) N. Gasparini, M. Salvador, S. Fladischer, A. Katsouras, A. Avgeropoulos, E. Spiecker, C. L. Chochos, C. J. Brabec and T. Ameri, *Adv. Energy Mater.*, 2015, **5**, 1501527; f) C. L. Chochos, R. Singh, M. Kim, N. Gasparini, A. Katsouras, C.

View Article Online
DOI: 10.1039/C7TA09224E

Kulshreshtha, V. G. Gregoriou, P. E. Keivanidis, T. Ameri, C. J. Brabec, K. Cho and A. Avgeropoulos, *Adv. Funct. Mater.*, 2016, **26**, 1840; g) C. L. Chochos, A. Katsouras, N. Gasparini, C. Koulogiannis, T. Ameri, C. J. Brabec and A. Avgeropoulos, *Macromol. Rapid Commun.*, 2017, **38**, 1600614; h) A. Katsouras, N. Gasparini, C. Koulogiannis, M. Spanos, T. Ameri, C. J. Brabec, C. L. Chochos and A. Avgeropoulos, *Macromol. Rapid Commun.*, 2015, **36**, 1778.

15. S. Beaupré and M. Leclerc, *J. Mater. Chem. A*, 2013, **1**, 11097.

16. N. Leclerc, P. Chávez, O. A. Ibraikulov, T. Heiser and P. Lévêque, *Polymers*, 2016, **8**, 11.

17. B. Carsten, F. He, H. J. Son, T. Xu and L. Yu, *Chem. Rev.*, 2011, **111**, 1493.

18. S. Roquet, A. Cravino, P. Leriche, O. Alévêque, P. Frère and J. Roncali, *J. Am. Chem. Soc.*, 2006, **128**, 3459.

19. S. Zhang, B. Yang, D. Liu, H. Zhang, W. Zhao, Q. Wang, C. He and J. Hou, *Macromolecules*, 2016, **49**, 120.

20. a) H. Zhou, L. Yang, A. C. Stuart, S. C. Price, S. Liu and W. You, *Angew. Chem. Int. Ed.*, 2011, **50**, 2995; b) Y. Wang, S. R. Parkin, J. Gierschner and M. D. Watson, *Org. Lett.*, 2008, **10**, 3307; c) X. Liu, Y. Sun, B. B. Y. Hsu, A. Lorbach, L. Qi, A. J. Heeger and G. C. Bazan, *J. Am. Chem. Soc.*, 2014, **136**, 5697; d) T. Okamoto, K. Nakahara, A. Saeki, S. Seki, J. H. Oh, H. B. Akkerman, Z. Bao and Y. Matsuo, *Chem. Mater.*, 2011, **23**, 1646; e) S. Yum, T. K. An, X. Wang, W. Lee, M. A. Uddin, Y. J. Kim, T. L. Nguyen, S. Xu, S. Hwang, C. E. Park and H. Y. Woo, *Chem. Mater.*, 2014, **26**, 2147; f) M.-C. Chen, Y.-J. Chiang, C. Kim, Y.-J. Guo, S.-Y. Chen, Y.-J. Liang, Y.-W. Huang, T.-S. Hu, G.-H. Lee, A. Facchetti and T. J. Marks, *Chem. Commun.*, 2009, **14**, 1846; g) J. Youn, P.-Y. Huang, Y.-W. Huang, M.-C. Chen, Y.-J. Lin, H. Huang, R. P. Ortiz, C. Stern, M.-C. Chung, C.-Y. Feng, L.-H. Chen, A. Facchetti and T. J. Marks, *Adv. Funct. Mater.*, 2012, **22**, 48; h) C. Kim, M.-C. Chen, Y.-J. Chiang, Y.-J. Guo, J. Youn, H. Huang, Y.-J. Liang, Y.-J. Lin, Y.-W.

View Article Online
DOI: 10.1039/C7TA09224E

Huang, T.-S. Hu, G.-H. Lee, A. Facchetti and T. J. Marks, *Org. Electron.*, 2010, **11**, 801; i) K. Reichenbacher, H. I. Süss and J. Hulliger, *Chem. Soc. Rev.*, 2005, **34**, 22.

21. a) L. Dou, J. Gao, E. Richard, J. You, C.-C. Chen, K. C. Cha, Y. He, G. Li and Y. Yang, *J. Am. Chem. Soc.*, 2012, **134**, 10071; b) Y. Lin, F. Zhao, Q. He, L. Huo, Y. Wu, T. C. Parker, W. Ma, Y. Sun, C. Wang, D. Zhu, A. J. Heeger, S. R. Marder and X. Zhan, *J. Am. Chem. Soc.*, 2016, **138**, 4955; c) K. Kawashima, Y. Tamai, H. Ohkita, I. Osaka and K. Takimiya, *Nat. Commun.*, 2015, **6**, 10085.

22. a) Z. He, C. Zhong, X. Huang, W.-Y. Wong, H. Wu, L. Chen, S. Su and Y. Cao, *Adv. Mater.*, 2011, **23**, 4636; b) X. Guo, N. Zhou, S. J. Lou, J. W. Hennek, R. P. Ortiz, M. R. Butler, P.-L. T. Boudreault, J. Strzalka, P.-O. Morin, M. Leclerc, J. T. L. Navarrete, M. A. Ratner, L. X. Chen, R. P. H. Chang, A. Facchetti and T. J. Marks, *J. Am. Chem. Soc.*, 2012, **134**, 18427; c) C. M. Proctor, J. A. Love and T.-Q. Nguyen, *Adv. Mater.*, 2014, **26**, 5957.

23. S. Albrecht, W. Schindler, J. Kurpiers, J. Kniepert, J. C. Blakesley, I. Dumsch, S. Allard, K. Fostiropoulos, U. Scherf and D. Neher, *J. Phys. Chem. Lett.*, 2012, **3**, 640.

24. T. M. Clarke and J. R. Durrant, *Chem. Rev.*, 2010, **110**, 6736.

25. I. A. Howard, R. Mauer, M. Meister and F. Laquai, *J. Am. Chem. Soc.*, 2010, **132**, 14866.

26. F. C. Jamieson, T. Agostinelli, H. Azimi, J. Nelson and J. R. Durrant, *J. Phys. Chem. Lett.*, 2010, **1**, 3306

27. A. Petersen, A. Ojala, T. Kirchartz, T. A. Wagner, F. Würthner and U. Rau, *Phys. Rev. B*, 2012, **85**, 245208.

28. C. G. Shuttle, B. O'Regan, A. M. Ballantyne, J. Nelson, D. D. C. Bradley, J. d. Mello and J. R. Durrant, *App. Phys. Lett.*, 2008, **92**, 093311.

29. F. Etzold, I. A. Howard, R. Mauer, M. Meister, T. D. Kim, K. S. Lee, N. S. Baek and F. Laquai, *J. Am. Chem. Soc.*, 2011, **133**, 9469.

View Article Online
DOI: 10.1039/C7TA09224E

30. S. Massip, P. M. Oberhumer, G. Tu, S. Albert-Seifried, W. T. Huck, R. H. Friend and N. C. Greenham, *J. Phys. Chem. C*, 2011, **115**, 25046.

31. M. Bernardi and J. C. Grossman, *Energy Environ. Sci.*, 2016, **9**, 2197.

32. P. A. Lane, P. D. Cunningham, J. S. Melinger, O. Esenturk and E. J. Heilweil, *Nat. Commun.*, 2015, **6**, 7558.

33. K. Yonezawa, H. Kamioka, T. Yasuda, L. Han and Y. Moritomo, *Appl. Phys. Express*, 2012, **5**, 042302.

34. J. Guo, Y. Liang, J. Szarko, B. Lee, H. J. Son, B. S. Rolczynski, L. Yu and L. X. Chen, *J. Phys. Chem. B*, 2010, **114**, 742.

35. R. Tautz, E. Como, T. Limmer, J. Feldmann, H. J. Egelhaaf, E. Hauff, V. Lemaur, D. Beljonne, S. Yilmaz, I. Dumsch, S. Allard and U. Scherf, *Nat. Commun.*, 2012, **3**, 970.

36. H. Loslein, T. Ameri, G. J. Matt, M. Koppe, H. J. Egelhaaf, A. Troeger, V. Sgobba, D. M. Guldi and C. J. Brabec, *Macromol. Rapid. Commun.*, 2013, **34**, 1090.

37. P. C. Y. Chow, S. Albert-Seifried, S. Gelinas and R. H. Friend, *Adv. Mater.*, 2014, **26**, 4851.

38. a) W. R. Mateker, J. D. Douglas, C. Cabanetos, I. T. Sachs-Quintana, J. A. Bartelt, E. T. Hoke, A. El Labban, P. M. Beaujuge, J. M. J. Fréchet and M. D. McGehee, *Energy Environ. Sci.*, 2013, **6**, 2529; b) T. Heumueller, W. R. Mateker, I. T. Sachs-Quintana, K. Vandewal, J. A. Bartelt, T. M. Burke, T. Ameri, C. J. Brabec and M. D. McGehee, *Energy Environ. Sci.*, 2014, **7**, 2974; c) J. K. Stille, *Angew. Chem. Int. Ed.*, 1986, **25**, 508; d) N. Grossiord, J. M. Kroon, R. Andriessen and P. W. M. Blom, *Org. Electron.*, 2012, **13**, 432; e) R. Rösch, D. M. Tanenbaum, M. Jørgensen, M. Seeland, M. Bärenklau, M. Hermenau, E. Voroshazi, M. T. Lloyd, Y. Galagan, B. Zimmermann, U. Würfel, M. Hösel, H. F. Dam, S. A. Gevorgyan, S. Kudret, W. Maes, L. Lutsen, D. Vanderzande, R. Andriessen, G. Teran-Escobar, M. Lira-Cantu, A. Rivaton, G. Y. Uzunoğlu, D. Germack, B. Andreasen, M. V. Madsen, K. Norrman, H. Hoppe and F. C. Krebs, *Energy Environ. Sci.*, 2012, **5**,

View Article Online
DOI: 10.1039/C7TA09224E

6521; f) E. Voroshazi, I. Cardinaletti, T. Conard and B. P. Rand, *Adv. Energy Mater.*, 2014, **4**, 1400848.

39. a) T Heumueller, T. M. Burke, W. R. Mateker, I. T. Sachs-Quintana, K. Vandewal, C. J. Brabec and M. D. McGehee, *Adv. Energy Mater.*, 2015, **5**, 1500111; b) A. Distler, T. Sauermann, H.-J. Egelhaaf, S. Rodman, D. Waller, K.-S. Cheon, M. Lee and D. M. Guldi, *Adv. Energy Mater.*, 2014, **4**, 1300693.

40. N. Gasparini, M. Salvador, S. Strohm, T. Heumueller, I. Levchuk, A. Wadsworth, J. H. Bannock, J. C. Mello, H.-J. Egelhaaf, D. Baran, I. McCulloch and C. J. Brabec, *Adv. Energy Mater.*, 2017, DOI: 10.1002/aenm.20170077.

41. a) M. O. Reese, A. M. Nardes, B. L. Rupert, R. E. Larsen, D. C. Olson, M. T. Lloyd, S. E. Shaheen, D. S. Ginley, G. Rumbles and N. Kopidakis, *Adv. Funct. Mater.*, 2010, **20**, 3476; b) S. Chambon, A. Rivaton, J.-L. Gardette and M. Firon, *Sol. Energy Mater. Sol. Cells*, 2007, **91**, 394; c) M. Manceau, A. Rivaton, J. L. Gardette, S. Guillerez and N. Lemaitre, *Sol. Energy Mater. Sol. Cells*, 2011, **95**, 1315; d) E. T. Hoke, I. T. Sachs-Quintana, M. T. Lloyd, I. Kauvar, W. R. Mateker, A. M. Nardes, C. H. Peters, N. Kopidakis and M. D. McGehee, *Adv. Energy Mater.*, 2012, **2**, 1351.

42. H. S. Lee, H. G. Song, H. Jung, M. H. Kim, C. Cho, J.-Y. Lee, S. Park, H. J. Son, H.-J. Yun, S.-K. Kwon, Y.-H. Kim and B. Kim, *Macromolecules*, 2016, **49**, 7844.

43. a) L. N. Inasaridze, A. I. Shames, I. V. Martynov, B. Li, A. V. Mumyatov, D. K. Susarova, E. A. Katz and P. A. Troshin, *J. Mater. Chem. A*, 2017, **5**, 8044; b) A. M. Rao, P. Zhou, K.-A. Wang, G. T. Hager, J. M. Holden, Y. Wang, W.-T. Lee, X.-X. Bi, P. C. Eklund, D. S. Cornett, M. A. Duncan and I. J. Amster, *Science*, 1993, **259**, 955; c) A. M. Rao, M. Menon, K.-A. Wang, P. C. Eklund, K. R. Subbaswamy, D. S. Cornett, M. A. Duncan and I. J. Amster, *Chem. Phys. Lett.*, 1994, **224**, 106; d) J. Wang, J. Enevold and L. Edman, *Adv. Funct. Mater.*, 2013, **23**, 3220; e) P. C. Eklund, A. M. Rao, P. Zhou, Y. Wang and J. M. Holden, *Thin Solid Films*, 1995, **257**, 185.

View Article Online
DOI: 10.1039/C7TA09224E

44. a) N. Li, J. D. Perea, T. Kassar, M. Richter, T. Heumueller, G. J. Matt, Y. Hou, N. S. Güldal, H. Chen, S. Chen, S. Langner, M. Berlinghof, T. Unruh and C. J. Brabec, *Nat. Commun.*, 2017, **8**, 14541; b) C. Zhang, A. Mumyatov, S. Langner, J. D. Perea, T. Kassar, J. Min, L. Ke, H. Chen, K. L. Gerasimov, D. V. Anokhin, D. A. Ivanov, T. Ameri, A. Osvet, D. K. Susarova, T. Unruh, N. Li, P. Troshin and C. J. Brabec, *Adv. Energy Mat.*, 2017, **7**, 1601204; c) J. D. Perea, S. Langner, M. Salvador, J. Kontos, G. Jarvas, F. Winkler, F. Machui, A. Görling, A. Dallos, T. Ameri and C. J. Brabec, *J. Phys. Chem. B*, 2016, **120**, 4431.

View Article Online
DOI: 10.1039/C7TA09224E

Table of Content Figure:

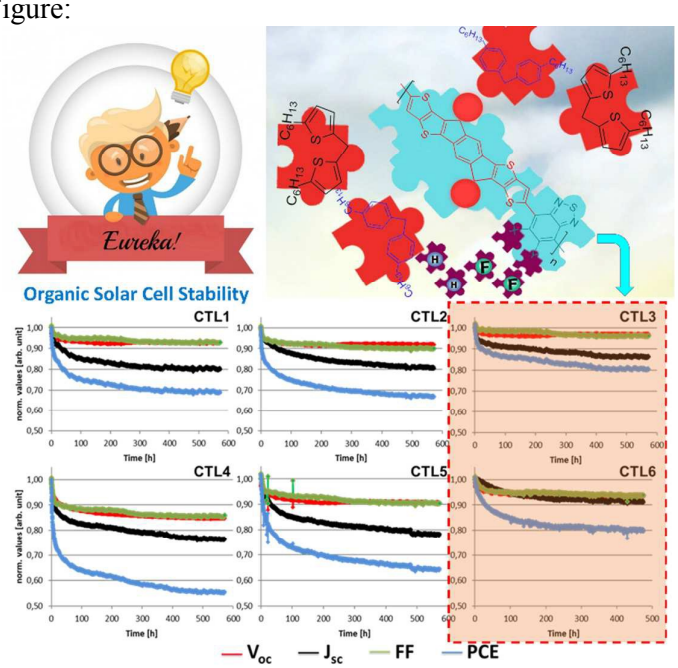

"The organic solar cell initial burn-in loss is substantially suppressed through the rational design of the polymeric semiconductor's chemical structure."